Whispering Vortices

A. Wallraff, A. V. Ustinov, V. V. Kurin,[†] I. A. Shereshevsky,[†] and N. K. Vdovicheva[†]

Physikalisches Institut III, Universität Erlangen-Nürnberg, D-91058 Erlangen, Germany
(Received 22 February 1999)

Experiments indicating the excitation of whispering-gallery-type electromagnetic modes by a vortex moving in an annular Josephson junction are reported. At relativistic velocities the Josephson vortex interacts with the modes of the superconducting stripline resonator giving rise to novel resonances on the current-voltage characteristic of the junction. The experimental data are in good agreement with analysis and numerical calculations based on the two-dimensional sine-Gordon model.

Whispering gallery modes are universal linear excitations of circular and annular resonators. They have first been observed in the form of a sound wave traveling along the outer wall of a walkway in the circular dome of St. Paul's Cathedral in London and were investigated by Lord Rayleigh [1] and others [2]. In the 2 m wide walkway, which forms a circular gallery of 38 m diameter about 40 m above the ground of the cathedral, the whispering of a person can be transmitted along the wall to another person listening to the sound on the other side of the dome. The investigations by Rayleigh led to the conclusion that the whisper of a person does excite acoustic eigenmodes of the circular dome which can be described using high order Bessel functions. This acoustic phenomenon lends its name "whispering gallery mode" to a number of similar, mostly electromagnetic excitations in circular resonators. Whispering gallery modes are of strong interest in microresonators used for ultrasmall lasers [3]. Most recently, circular resonators with small deformations, in which chaotic whispering gallery modes were observed, attracted a lot of attention [4]. Here we describe the experimental observation of electromagnetic whispering gallery modes excited by a vortex moving in an annular Josephson junction of diameter less than 100 μm.

A long Josephson junction is an intriguing nonlinear wave propagation medium for the experimental study of the interaction between linear waves and solitons [5]. In this Letter, we report the excitation of whispering-gallery-type electromagnetic modes by a topological soliton (Josephson vortex) moving at relativistic velocities in a wide annular Josephson junction. We make use of the same Josephson vortex for both exciting and detecting the whispering gallery mode. These modes are manifested by their resonant interaction with the moving vortex, which results in a novel fine structure on the current-voltage characteristic of the junction. Our experiments are consistent with the recently published theory [6] based on the two-dimensional sine-Gordon model. We present numerical calculations based on this model, which show good agreement with experiments.

Electromagnetic waves in an annular Josephson junction are described by the perturbed sine-Gordon equation (PSGE) for the superconducting phase difference ϕ between the top and bottom superconducting electrodes of the junction [5]. The Josephson vortex, often also called fluxon, corresponds to a twist over 2π in ϕ. It carries a magnetic flux equal to the magnetic flux quantum $\Phi_0 = h/2e = 2.07 \times 10^{-15}$ V s. Physically, this flux is induced by a vortex of the screening current flowing across the junction barrier. Linear excitations in this system are Josephson plasma waves that account for small amplitude oscillations in ϕ. The maximum phase velocity of electromagnetic waves in such a junction is the Swihart velocity given by $c_0 = \lambda_J \omega_p$, where λ_J is the Josephson length, and ω_p is the plasma frequency [5]. In zero external magnetic field, the PSGE for an annular Josephson junction of width $w < \lambda_J$ can be written as

$$\left(\nabla^2 - \frac{\partial^2}{\partial t^2}\right)\phi - \sin\phi = \gamma + \alpha\,\frac{\partial\phi}{\partial t} - \beta\nabla^2\frac{\partial\phi}{\partial t}, \quad (1)$$

where space and time are normalized by λ_J and ω_P^{-1}, respectively. In Eq. (1), $\nabla^2 - \partial^2/\partial t^2$ is the D'Alembert wave operator, $\sin\phi$ is the nonlinear term due to the phase-dependent Josephson current, and γ is the normalized bias current. The damping terms $\alpha\,\partial\phi/\partial t$ and $\beta\nabla^2\partial\phi/\partial t$ are inversely proportional to the quasiparticle resistance across the junction barrier and to the quasiparticle impedance of the electrodes, respectively. For the junctions of width $w < \lambda_J$ considered in this paper, a homogeneously distributed bias current γ as in Eq. (1) is justified. In contrast, for junctions with $w > \lambda_J$ the bias current may contribute to the boundary conditions of Eq. (1) [7].

A vortex steadily moving at a velocity u driven by the Lorentz force due to the bias current γ generates a voltage $V \propto u$ across the Josephson junction. This voltage can be monitored in experiment. The radiation associated with the time-dependent fields described by Eq. (1), i.e., the magnetic field $H \propto |\nabla\phi|$ and the electric field $E \propto \partial\phi/\partial t$, can be measured either directly (for certain junction geometries) or through its interaction with the moving vortex.

In contrast to most of the previous experiments focusing on quasi-one-dimensional annular Josephson junctions,

we investigate comparatively wide, effectively two-dimensional junctions. We have fabricated a set of five annular Josephson junctions $(A, \ldots, E)$ with the ratio $\delta = r_i/r_e$ between the inner radius r_i and the fixed outer radius $r_e = 50$ μm being varied between $\delta = 0.94$ and $\delta = 0.60$ (see Table I). The junctions are made at Hypres Inc. [8] using Nb-Al/AlO$_x$-Nb trilayer technology and employ the standard biasing geometry [9] as shown in Fig. 1. Because of the fabrication technology, the junction area is surrounded by a small passive region about 2 μm wide, which is omitted from Fig. 1 for clarity. In the passive region, the top and bottom electrodes are separated by a 200 nm thick SiO$_2$ layer, which acts as a small stripline in parallel to, but with electrical parameters different from, the junction itself.

All junctions show a homogeneous bias current distribution, inferred from the large value of the vortex-free critical current at zero field, which is close to the theoretical limit. Their critical current density is $j_c \approx 160$ A cm^{-2}, and the London penetration depth is $\lambda_L \approx 90$ nm at 4.2 K. The thicknesses of the top and the bottom superconducting electrode are both well in excess of λ_L. Accordingly, the characteristic parameters are estimated as $\lambda_J \approx 30$ μm and $\nu_p \equiv \omega_p/2\pi \approx 50$ GHz. All presented measurements were done at $T = 4.2$ K using a well shielded low noise measurement setup.

We could realize single- and multiple-vortex states repeatedly and reproducibly in any of the junctions. Vortices were trapped by applying a small bias current during cooling down from the normal to the superconducting state. Single-vortex states are identified as the lowest quantized voltage step observed on the current-voltage characteristics. Also, a characteristic change of the critical current modulation with magnetic field accompanied by a suppression of the critical current by a factor of more than 100 at zero field, as reported earlier [10], was observed when a vortex was trapped in the junction.

In Fig. 2 the single-vortex characteristics of the junctions A to E are shown. The current scale is normalized by the flux-free zero-field critical current of each junction. The voltage of each characteristic is multiplied by a factor $\xi = c_0/\bar{c}_0$ (see Table I) calculated using the approach by Lee et al. [11], in order to substract the effect of a small
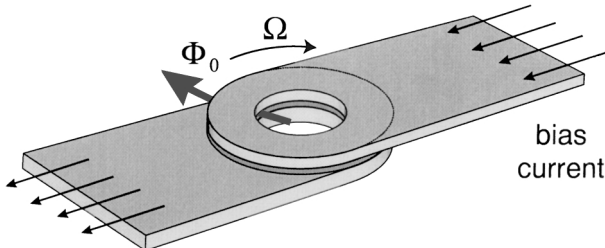

FIG. 1. Geometry of the annular Josephson junction. The direction of the angular velocity Ω of the vortex (Φ_0) under the action of the bias current is indicated.

TABLE I. Geometrical parameters of the annular Josephson junctions used in experiment. The outer radius of every junction is $r_e = 50$ μm. $w = r_e - r_i$ is the junction width.

Junction	A	B	C	D	E
r_i [μm]	47	45	42	35	30
w [μm]	3	5	8	15	20
$\delta = r_i/r_e$	0.94	0.90	0.84	0.70	0.60
$\xi = c_0/\bar{c}_0$	0.70	0.78	0.85	0.91	0.94

passive region. c_0 ($\bar{c}_0$) is the wave velocity in the junction neglecting (including) the passive region.

A striking novel feature noticed in Fig. 2 is the fine structure on the vortex resonance which appears with increasing the junction width. The fine structure is most clearly visible for the widest junction E (see inset of Fig. 2). We argue that the observed fine structure can be well understood as due to the interaction of the moving vortex with the linear whispering gallery modes [6]. The linear modes of the annular Josephson junction resonator are solutions to the inhomogeneous D'Alembert equation in the polar coordinates (r, θ):

$$\left(\frac{1}{r} \frac{\partial}{\partial r} r \frac{\partial}{\partial r} + \frac{1}{r^2} \frac{\partial^2}{\partial \theta^2} - \frac{\partial^2}{\partial t^2} - 1 \right) \phi^{(\mathrm{lin})} = 0, \quad (2)$$

which is found from Eq. (1) neglecting all perturbations $(\gamma, \alpha \partial/\partial t, \beta \nabla^2 \partial \phi/\partial t)$ and approximating the nonlinearity as $\sin\phi \approx \phi$ to take into account the gap in the plasmon excitation spectrum. In zero external magnetic field, the boundary conditions

$$\frac{\partial \phi^{(\mathrm{lin})}}{\partial r} (r = r_i, r_e) = 0 \quad (3)$$

have to be fulfilled. In terms of the electromagnetic waves in the junction, Eq. (3) corresponds to a total internal reflection condition. For large angular wave numbers
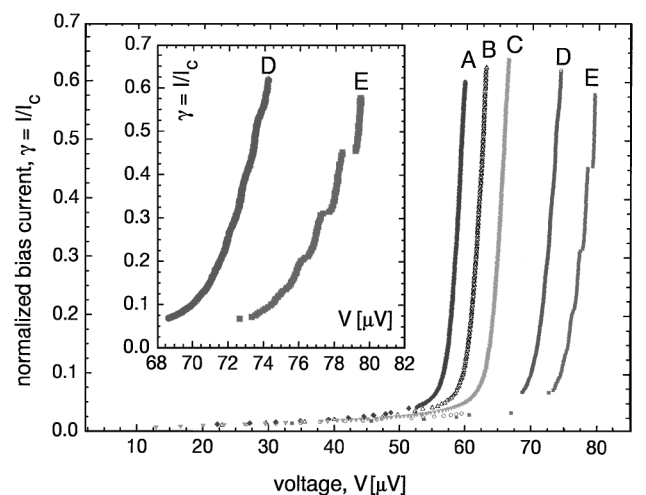

FIG. 2. Experimental normalized current-voltage characteristics of single-vortex states in junctions A to E. An enlargement of the high voltage region of the resonances in junctions D and E is shown in the inset.

$k \gg 1$ and wide junctions $\delta \ll 1$ a solution to (2) is given by

$$\phi_k^{(\text{lin})}(r, \theta, t) = A J_k(\omega_k r) \exp(ik\theta) \exp(i\omega_k t), \qquad (4)$$

where A is an arbitrary amplitude factor, J_k is the Bessel function of the first kind, and ω_k is the angular frequency associated with the mode k satisfying the boundary condition (3) at the external radius. By calculating the dependence of ω_k on k, one obtains the dispersion relation of whispering gallery modes in the annular junction.

The resonance condition between the angular frequency Ω of the vortex rotation in the ring and the characteristic frequency ω_k of a whispering gallery mode can be expressed as

$$\Omega = \omega_k/k . \qquad (5)$$

In a dispersion diagram, Eq. (5) determines the crossing points between the straight dispersion line of the vortex $\omega^{(\text{v})} = \Omega k$ and the dispersion curve $\omega^{(\text{lin})} = \omega_k$ of the linear modes. At low enough damping, a vortex moving at the angular frequency Ω comes into resonance with a whispering gallery mode of wave number k. If the spacing in Ω between the resonances for different k is large enough, this effect can be observed as fine structure resonances on the single-vortex current-voltage characteristic of a wide annular Josephson junction. The increase of the excited wave number k with decrease of the vortex velocity is a characteristic feature of the interaction between the Josephson vortex and the whispering gallery modes of the junction. This property is clearly manifested in our numerical calculations presented below.

To confirm the above interpretation of our experimental results, we performed direct numerical simulations of Eq. (1) in polar coordinates with the boundary conditions (3) using our junction parameters (see Table I). We calculated current-voltage characteristics $V(\gamma) = \Phi_0 \Omega(\gamma) \omega_p/(2\pi)$ and two-dimensional phase profiles $\phi(r, \theta, t)$ for various bias points using a plasma frequency of $\omega_p/2\pi = 52.4$ GHz determined from experimental data. The damping parameter $\alpha = 0.03$ was chosen close to its estimated experimental value at $T = 4.2$ K; β here was set to 0. The calculated characteristics for junctions A to E are plotted in Fig. 3. Clearly, the fine structure on the current-voltage characteristics of the wide junctions D and E is very well reproduced in the simulation. Figure 4 shows the phase profiles at bias points on subsequent fine structure resonances of junction E. Evidently, a clear whispering gallery structure is found here. With decreasing bias, the increase of the angular wave number of the mode from resonance to resonance is observed.

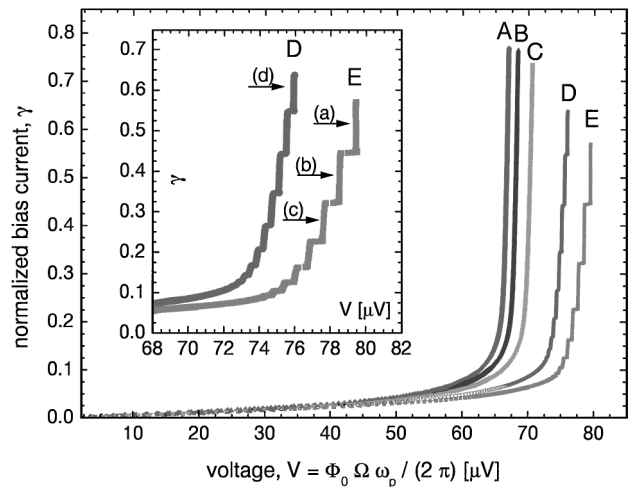Using the resonance condition (5) and the proportionality between the angular frequency of the vortex Ω and

FIG. 3. Numerically calculated current-voltage characteristics $V(\gamma)$ for junctions A to E. In the inset the characteristics of junctions D and E are shown on an enlarged scale. Arrows indicate the bias points used to obtain the phase profiles shown in Fig. 4.

the voltage V measured in experiment, the fine structure resonances can be fitted according to the formula

$$V = \Phi_0 \frac{\omega_p}{2\pi} \Omega = \Phi_0 \frac{\omega_p}{2\pi} \frac{\omega_k}{k} , \qquad (6)$$

where k is an integer. In the limit of $\delta \ll 1$ and $k \gg 1$ the linear mode spectrum can be analytically approximated as $\omega_k = r_e^{-1}(k + 0.808\, k^{1/3})$ [6]. More accurately, we have calculated the values of ω_k numerically solving Eq. (2) with the boundary conditions (3). The best fit to the experimental data is found for the plasma frequency
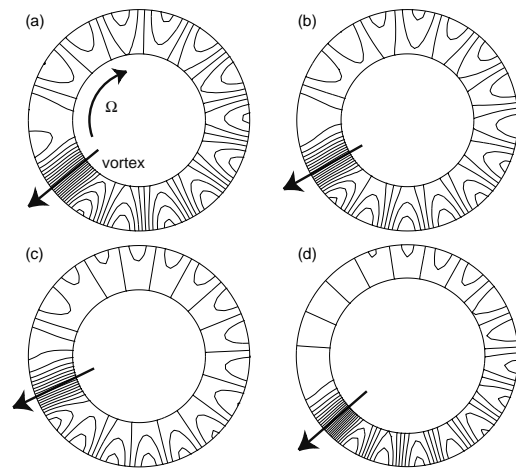

FIG. 4. Phase profiles $\phi(r, \theta)$ at bias γ equal to (a) 0.5, (b) 0.4, and (c) 0.3 on the single-vortex resonance of junction E and at $\gamma = 0.6$ for junction D. Plotted are lines of constant phase; their high density corresponds to a large gradient of phase and, hence, a large magnetic field. The position of the vortex is indicated by an arrow. The whispering gallery modes with angular wave number k equal to (a) 7, (b) 8, (c) 9, and (d) 9 are observed.
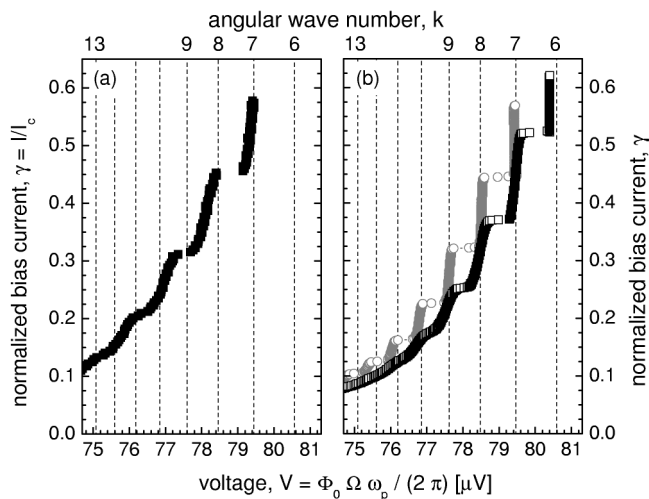
153

FIG. 5. (a) Upper part of experimental single-vortex current-voltage characteristic of junction E. (b) Simulated current-voltage characteristic of this junction for $\alpha = 0.03$, $\beta = 0$ (open circles) and $\alpha = 0.02$, $\beta = 0.0012$ (open squares). The calculated resonance voltages are indicated by vertical dotted lines and marked by the corresponding wave number k.

$\omega_p/2\pi = 52.4$ GHz and the wave number $k = 7$ for the highest voltage resonance (see Fig. 5a). This value of k is exactly the one found for the highest resonance in numerical simulations (see Fig. 4a). The voltages of the resonances found in simulation (Fig. 5b) are close to the ones calculated from the dispersion relation (dotted lines). The current-voltage characteristic of junction E simulated for the damping parameters $\alpha = 0.02$ and $\beta = 0.0012$ is shown in Fig. 5b (open squares). Clearly, taking into account the quasiparticle surface losses ($\propto \beta$) leads to a larger differential resistance of the resonance, which closely resembles the experimental data in Fig. 5a.

Considering the resonance condition Eq. (5) and the dispersion of the linear modes ω_k, it can be shown that the density of resonances in voltage and the wave number of the lowest excited mode increase with decreasing junction width $w = r_e - r_i$. This fact was verified by numerical calculations for junction D, where the lowest mode number excited on the top of the resonance was found to be $k = 9$ (see Fig. 4d). For very narrow rings, no fine structure is observed in experiment and in simulation, due to the overlapping of neighboring resonances in the presence of damping.

The origin of the observed fine structure has also been confirmed to be due to the interaction of the vortex with the whispering gallery modes of the junction by investigating its dependence on temperature, number of trapped vortices, and external magnetic field. At high temperatures, no whispering gallery resonances are excited due to the large intrinsic damping, i.e., no fine structure is observed. Decreasing the temperature below 4.2 K, fine structure is observed in all samples A to E; also the differential resistance of the resonances decreases with temperature. Moreover, we found that the voltages of the fine structure resonances scale with the number n of moving vortices (or vortex/antivortex pairs). Therefore, for $n > 1$ the fine structure gets clearly resolved in voltage and also more pronounced, because several vortices coherently pump the whispering gallery mode. No dependence of the fine structure step voltage positions on small external magnetic fields was noticed. We have also investigated more narrow annular junctions with a wide idle region both experimentally and theoretically [12]. In this case, the spectrum of the whispering gallery modes (and, thus, of the fine structure) is strongly influenced by the geometry and the electrical properties of the passive region. The fine structure recently reported in Ref. [13] appears to be consistent with our observations.

In summary, we have presented experimental and numerical evidences for the excitation of whispering gallery modes by vortices moving in wide annular junctions. This novel effect has been observed at sufficiently low damping for annular junctions in a wide range of electrical and geometrical parameters. It is very robust with respect to small external perturbations such as variations in bias current density, boundary conditions, or junction inhomogeneities. The resonance frequencies have been calculated, and quantitative agreement with experimental data and numerical simulations better than one percent has been reached. Thus, the vortices appear to whisper (generate radiation) at frequencies between 250 and 450 GHz in the annular whispering gallery of 100 μm diameter.

[†]Institute for Physics of Microstructure (RAS), GSP-105, 603600 Nizhny Novgorod, Russia.
[1] L. Rayleigh, Philos. Mag. **27**, 100 (1914).
[2] J. Walker, Sci. Am. **239**, 146 (1978).
[3] S. L. McCall *et al.,* Appl. Phys. Lett. **60**, 289 (1991).
[4] C. Gmachl *et al.,* Science **280**, 1556 (1998).
[5] A. V. Ustinov, Physica (Amsterdam) **123D**, 315 (1998).
[6] V. V. Kurin *et al.,* Phys. Rev. Lett. **80**, 3372 (1998).
[7] N. Martucciello and R. Monaco, Phys. Rev. B **53**, 3471 (1996).
[8] Hypres Inc., Elmsford, NY 10523.
[9] A. Davidson *et al.,* Phys. Rev. Lett. **55**, 2059 (1985).
[10] I. V. Vernik *et al.,* J. Appl. Phys. **81**, 1335 (1997).
[11] G. Lee and A. Barfknecht, IEEE Trans. Appl. Supercond. **2**, 67 (1992).
[12] A. Wallraff *et al.,* Physica B, Proceedings of the LT-22, Helsinki (to be published).
[13] N. Martucciello *et al.,* Phys. Rev. B **57**, 5444 (1998).